iScience

CellPress
OPEN ACCESS

Article

Bleaching-free, lignin-tolerant, high-yield production of nanocrystalline cellulose from lignocellulosic biomass

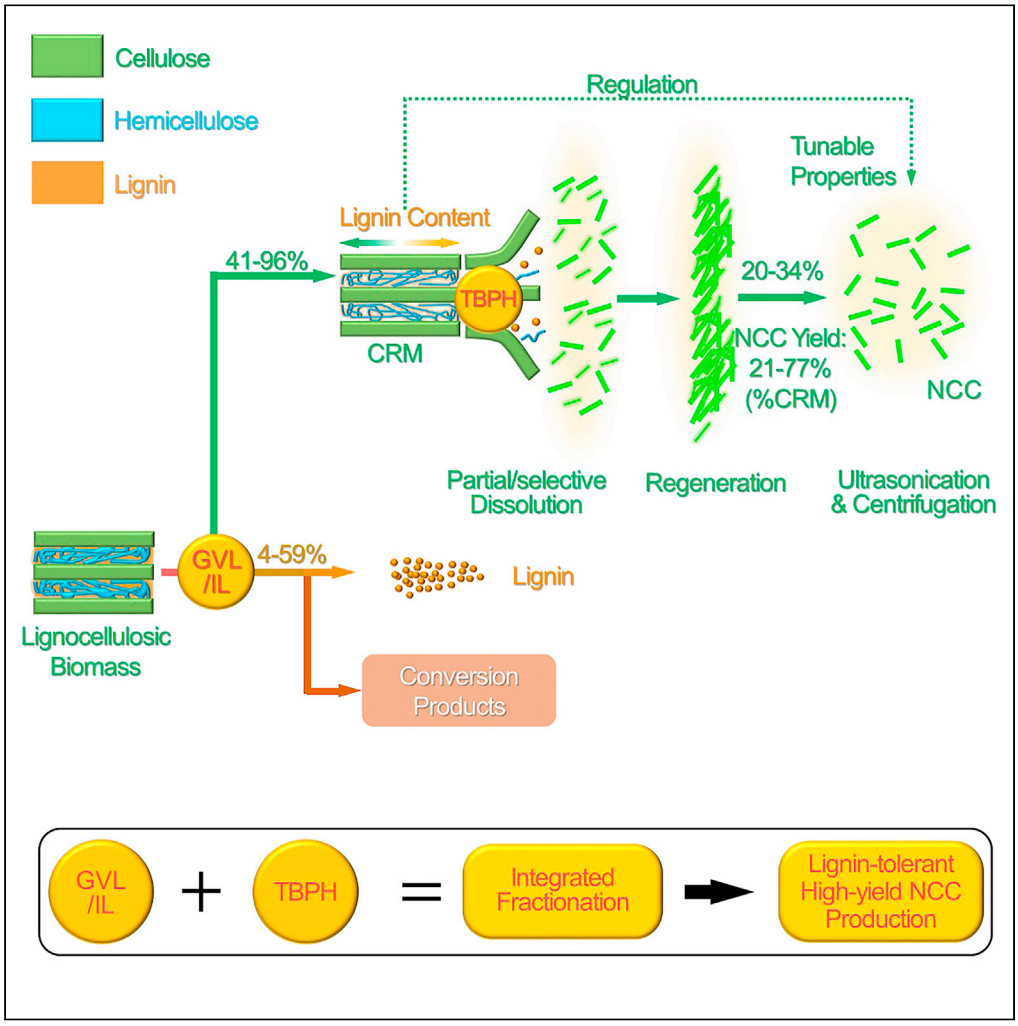

Zipeng Li, Di Xie, Weizhi Zhu, ..., Jianping Sun, Yiqiang Wu, Fangchao Cheng

fangchaocheng@gxu.edu.cn

Highlights

A bleaching-free, lignin-tolerant strategy for high-yield NCC production was used

The strategy combined wood fractionation with partial dissolution of cellulose

The process can tolerate a lignin content of 21.2 wt % in cellulose-rich materials

The process provided a high NCC yield of 76.6 wt %, which was 34.3 wt % of wood

Li et al., iScience 26, 105771
January 20, 2023
https://doi.org/10.1016/j.isci.2022.105771

iScience

CellPress
OPEN ACCESS

Article

Bleaching-free, lignin-tolerant, high-yield production of nanocrystalline cellulose from lignocellulosic biomass

Zipeng Li,[1,3] Di Xie,[1,3] Weizhi Zhu,[1] Hongjie Wang,[1] Tulong Ouyang,[1] Jianping Sun,[1] Yiqiang Wu,[2] and Fangchao Cheng[1,2,4,*]

SUMMARY

Nanocrystalline cellulose (NCC) preparation in an integrated fractionation manner is expected to solve the problems of low yield and environmental impact in the traditional process. An integrated fractionation strategy for NCC production from wood was developed through catalytic biomass fractionation, the partial dissolution of cellulose-rich materials (CRMs) in aqueous tetrabutylphosphonium hydroxide, and short-term ultrasonication. The presented process could tolerate a high CRM lignin content of 21.2 wt % and provide a high NCC yield of 76.6 wt % (34.3 wt % of the original biomass). The increase in the CRM lignin content decreased the NCC yield, facilitated the crystal transition of NCC from cellulose I to cellulose II, and showed no apparent effects on the NCC morphology. A partial/selective dissolution mechanism is proposed for the presented strategy. This study provided a promising efficient fractionation-based method toward comprehensive and high-value utilization of lignocellulosic biomass through effective delignification and high-yield NCC production.

INTRODUCTION

Lignocellulosic biomass, which is composed of cellulose, hemicellulose, lignin, and minor amounts of extractives, is one of the most abundant resources in nature.[1] Nanocrystalline cellulose (NCC), one of the most important products extracted from lignocellulosic biomass, possesses a unique nanostructure and excellent physical-mechanical properties and shows wide application prospects in the fields of fine chemical engineering, biomedicine, and advanced materials.[2–5] In the conventional production process of NCC, commercial cellulosic materials, such as microcrystalline cellulose and pulp, are mainly employed as the starting materials.[6] However, in the pulping process, most of the other components (e.g., hemicellulose and lignin) are not used effectively, and the utilization efficiency of components needs to be improved.[7] In recent years, NCC production directly from lignocellulosic biomass has attracted extensive attention,[8] because it conforms to the emerging integrated biorefinery concept and enables the realization of comprehensive and efficient biomass utilization.[9,10]

The NCC production from lignocellulosic biomass usually involves delignification, bleaching of cellulose-rich materials (CRMs), and the nanocrystallization of purified cellulosic materials.[11] Zhang and Liu[12] prepared NCC through irradiation oxidation and organosolv solubilization of eucalyptus wood using various organic solvents and a NaClO/NaOH system. The fractionation and bleaching of lignocellulosic biomass can break the lignin-carbohydrates complex (LCC), decompose the lignin, and improve the nanocrystallization efficiency.[13] However, these processes usually involve complicated treatment processes, and how to reduce their environmental impact and energy consumption is an important issue.[14] Recently, γ-valerolactone (GVL), a sustainable chemical derived from lignocellulosic biomass, has been considered as a green solvent in chemical processes.[1]

In addition to the fractionation and bleaching processes, the cellulose nanocrystallization process can also significantly influence the morphology and physicochemical properties of NCC.[15] Acidic hydrolysis has been regarded as one of the most important chemical methods for cellulose nanocrystallization; it can selectively hydrolyze the amorphous region of cellulose to produce nanoscale crystals.[16] The mechanical treatment of cellulose, including high-pressure shearing, high-pressure homogenization, and

[1]Guangxi Key Laboratory of Processing for Nonferrous Metallic and Featured Materials, School of Resources, Environment and Materials, Guangxi University, Nanning 530004, China

[2]College of Material Science and Engineering, Central South University of Forestry and Technology, Changsha 410004, China

[3]These authors contributed equally

[4]Lead contact

*Correspondence: fangchaocheng@gxu.edu.cn

https://doi.org/10.1016/j.isci.2022.105771

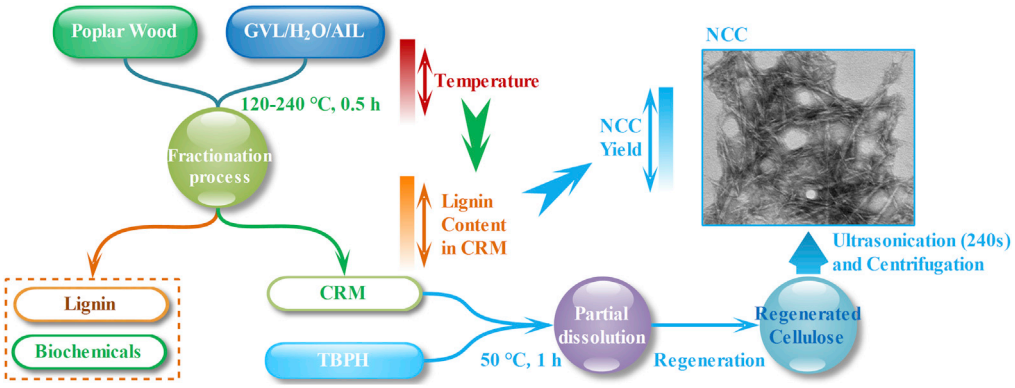

Figure 1. Partial dissolution-based integrated fractionation strategy for NCC production

ultrasonication, can also be combined with the hydrolysis process to prepare NCC.[17] The above methods have been widely used to disassemble cellulose for NCC preparation, whereas the problems of high energy consumption, high environmental impact, and low NCC yield still hinder the efficient and large-scale production of NCC.[11]

A cellulose-dissolving system (e.g., ionic liquids, ILs) can effectively deconstruct the hydrogen bonding network and dissolve cellulose. It can be used to improve the NCC production efficiency and reduce the energy consumption.[18] For example, 1-ethyl-3-methylimidazolium acetate, an effective IL for cellulose dissolution, can produce surface-acetylated NCC through the partial dissolution of lignocellulosic biomass and subsequent ultrasonic treatment.[19] However, the disadvantages of imidazole-based ILs in the cellulose dissolution, such as high viscosity and long treatment time, limit the application of ILs in NCC preparation.[20] In addition, the existence of lignin and hemicellulose in cellulosic raw materials has been proved to greatly influence the NCC properties, and higher lignin content usually leads to low NCC yield.[21,22] In recent years, it is found that the aqueous tetrabutylphosphonium hydroxide (TBPH) with strong proton receptivity can dissolve and fractionate cellulose from primitive lignocellulosic materials under mild conditions.[23] Thus, the hypothesis of this study was that integrating the lignocellulose dissolution into the fractionation processes for NCC production, which will be conducive to the simultaneous realization of high-value comprehensive utilization of biomass and high-yield NCC acquisition.

In this study, cellulose nanocrystallization based on partial dissolution was integrated into the fractionation process of biomass to reduce the environmental impact, promote the comprehensive utilization of biomass components, and achieve efficient NCC production in an integrated fractionation manner (Figure 1). This study can promote the efficient and comprehensive conversion of biomass into biochemicals and advanced materials by reducing environmental impact, enhancing the selective fractionation and dissolution, and improving production efficiency.

RESULTS AND DISCUSSION

Fractionation results

The fractionation results of poplar under different treatment temperatures are illustrated in Figure 2. With the increase in the temperature from 120 °C to 240 °C, the CRM yield gradually decreased from 95.8% to 41.1%, and the lignin yield increased from 1.5% to 13.8%. Meanwhile, the mass loss increased from 2.7% to 45.1% as the temperature increased (Figure 2A). The treatment temperature significantly influenced the fractionation results. A previous study has also confirmed the effect of temperature on the biomass fractionation process, and it is found that high temperature led to high delignification rate and facilitated the conversion of carbohydrates, resulting in a low CRM yield and high mass loss.[24] In the current study, the lignin content in CRM varied from 21.2% to 3.4% at different temperatures, leading to a delignification rate ranging from 8.1% to 93.7% (Figure 2B). Based on these fractionation processes at different temperatures, a series of CRM samples with different lignin contents were successfully prepared. The scanning electron microscopy results of CRM also indicate that both the poplar powder and CRMs were rod-shaped particles, and the increase in temperature greatly reduced the CRM particle dimensions, with the particle

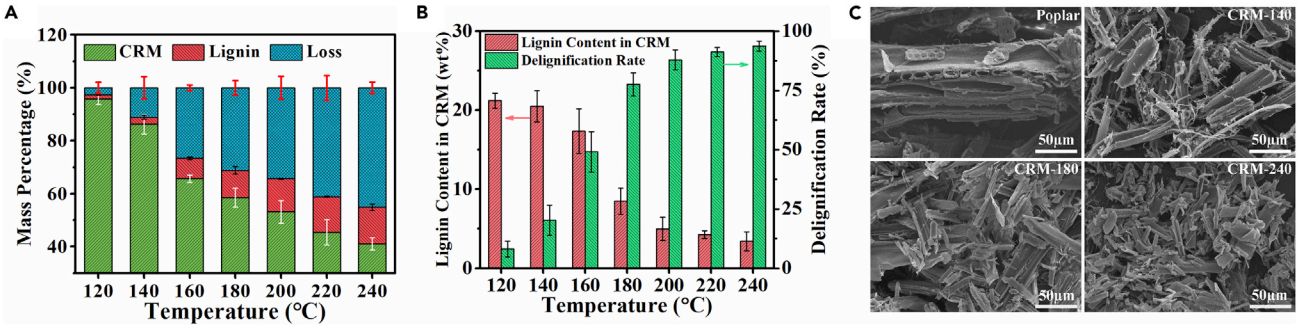

Figure 2. Fractionation results and SEM images

(A) mass percentage of components and loss.

(B) lignin content in CRM and the corresponding delignification rate.

(C) SEM images of poplar and different CRM samples.

diameter ranging from tens or even hundreds of microns to several microns (Figure 2C). In addition, the cell wall structure of poplar gradually disappeared as the treatment temperature increased. The higher temperature can lead to a higher degree of lignin dissolution and carbohydrate conversion, thereby resulting in the dissociation of the poplar cell wall and the decrease in particle size.[25] It has also been reported that most of hemicellulose was catalytically decomposed into biochemical during the organosolv process.[24] Consequently, the presented strategy enabled the comprehensive utilization of biomass components by lignin dissolution/separation and hemicellulose conversion, and the as-prepared CRMs can be subsequently converted into NCC through partial dissolution in TBPH and short-term ultrasonication, which provided an integrated fractionation method for the comprehensive conversion of biomass into high-performance materials and biochemicals.

NCC production results

The results of NCC yield (%CRM) and NCC extraction rate (%poplar) for the NCC production processes with different CRM samples (from CRM-120 to CRM-240) are presented in Figure 3A. The lignin content in CRM significantly influenced the NCC yield. As the CRM lignin content decreased from 21.2% to 3.4%, the NCC yield remarkably increased, from 20.8% to 76.6%. There are two possible reasons for this phenomenon: First, the presence of lignin increased the recalcitrant characteristics of cellulose materials, which was not conducive to the dissociation of the cellulose hydrogen bonding network.[22] Second, most of the lignin would be dissolved during the TBPH treatment process,[23] and only a small amount of lignin entered the NCC; thus, the higher lignin content led to a lower NCC yield because of the removal of lignin.

As discussed in fractionation results, a higher treatment temperature should be adopted to achieve a lower CRM lignin content, but this will also lead to a lower CRM yield. Meanwhile, considering the effect of the lignin content on the NCC yield, although the low lignin content in CRM (e.g., 3.4% for CRM-240) can greatly improve the NCC production efficiency (76.6% for NCC-240), the low CRM yield (41.1%) will also reduce the comprehensive biomass utilization rate. Herein, the NCC extraction rate, which was represented by the ratio of the NCC mass to the mass of the original poplar, was adopted to investigate the comprehensive utilization rate of biomass in the NCC production process (Figure 3A). The NCC extraction rate first increased and then decreased with decreasing CRM lignin content. The NCC production using CRM-200 as the raw material gave the highest NCC extraction rate (34.3%), which meant 34.3% of the original poplar was extracted as NCC. In addition, CRM-180 also resulted in a promising NCC extraction rate (33.5%). Considering the lower treatment temperature of CRM-180, it can also be regarded as one of the best raw materials for the NCC production process, aiming at the comprehensive utilization of biomass. During the fractionation-based NCC production process, lignocellulosic biomass was fractionated into NCC and lignin, and most of the hemicellulose could be converted into low-molecular-weight chemicals, as reported in the previous study[24]; thus, the process enables comprehensive biomass utilization, which conforms to the concept of integrated biorefinery.[10]

The TEM results confirmed that the resultant NCC exhibited rod-like morphology (Figures 3C–3F), which was similar to that obtained via acid hydrolysis.[26] The statistical results of NCC size based on TEM

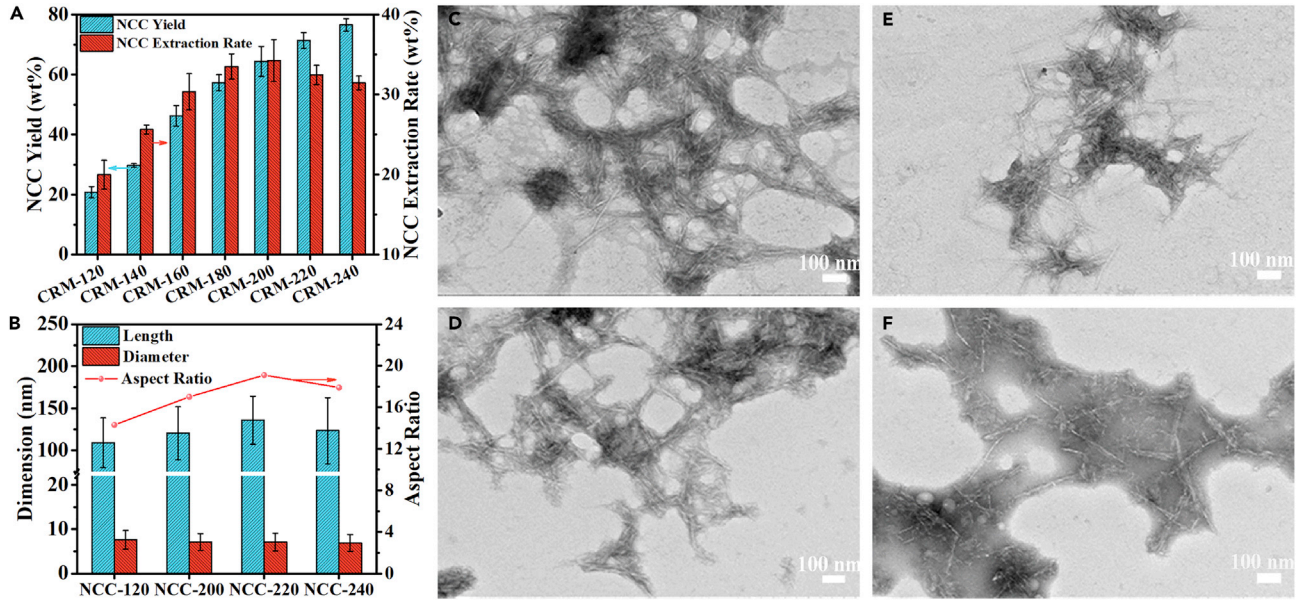

Figure 3. NCC production results

(A) NCC yield and extraction rate results for production processes using different CRMs; (B) Size distribution of NCC produced with different CRMs; TEM images of NCC-120 (C), NCC-200 (D), NCC-220 (E) and NCC-240 (F).

images are presented in Figure 3B. The lignin content in CRM showed limited influence on the NCC particle dimensions, which led to diameters around 7 nm and varied lengths (109–136 nm) and aspect ratios (14.3–19.1) of NCC. This should be mainly because of the high lignin solubility in TPBH solution.[27] During the NCC production processes, lignin in CRM can be readily dissolved in the solvent, and it would not greatly affect the cellulose dissociation and dissolution. Consequently, the NCC production based on TBPH treatment revealed high lignin tolerance, which can accommodate cellulose materials with a lignin content of over 20%.

FT-IR analysis

The FT-IR spectra of poplar and CRM showed significant differences in the characteristic bands of hemicellulose and lignin at 1736 cm^{-1} (acetyl group, mainly in hemicellulose), 1595 cm^{-1} (C=C stretching in lignin), 1505 cm^{-1} (aromatic skeleton in lignin), 1462 cm^{-1} (C-H deformation in lignin), and 1247 cm^{-1} (C-*O*-C stretching in lignin).[28,29] With the increase in the treatment temperature, the intensities of these bands decreased until the bands disappeared, indicating the increasing removal of hemicellulose and lignin, which accords with the fractionation results (Figure 4A). The characteristic bands of cellulose in the spectra of different CRMs exhibited no significant change except for the enhanced characteristic band of hydrogen bonding (3348 cm^{-1}) at the high treatment temperature.[29] This indicates that the chemical structure of cellulose was not significantly affected by the fractionation process, and the removal of hemicellulose and lignin would enhance the hydrogen bonding network of cellulose.

The FT-IR spectra of NCC revealed that NCC prepared with different CRMs showed no significant difference in chemical structure (Figure 4B). The blueshift of the absorption band around 3460 cm^{-1}, which is attributed to O-H stretching vibration, indicates that the hydrogen bonding and crystalline structure of cellulose changed after the TBPH treatment.[30] The absorption peak of hemicellulose at 1736 cm^{-1} was absent in the spectra of all NCC samples, indicating that hemicellulose was further removed after the TBPH treatment. Moreover, low-intensity absorption peaks of lignin at 1595 cm^{-1}, 1505 cm^{-1}, and 1462 cm^{-1} were also present in the spectra of NCC-120 and NCC-140, revealing that the resultant NCC still contained a small amount of lignin.[29] However, these bands were absent in the spectra of the NCC produced with CRM obtained at higher temperatures. These results indicate that the TBPH treatment can largely remove hemicellulose and lignin and change the cellulose crystalline structure.

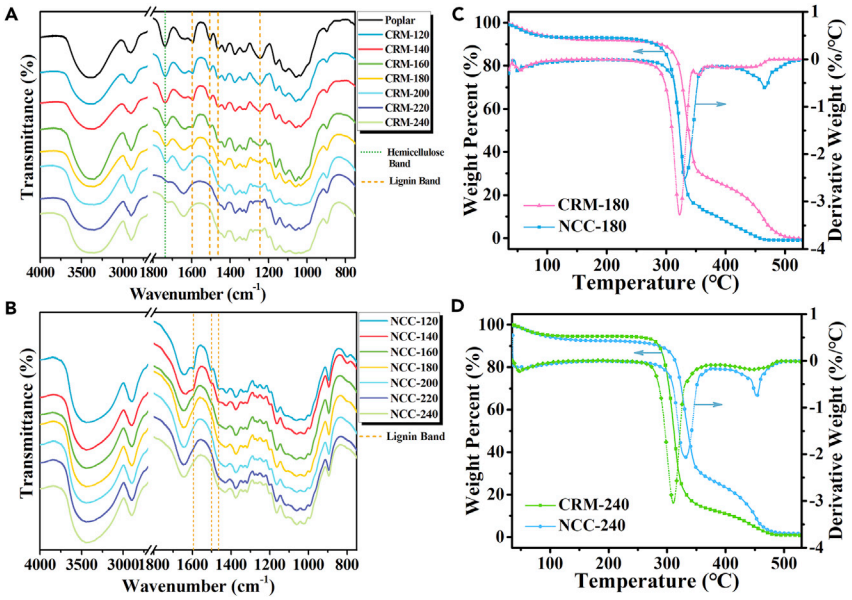

Figure 4. Results of chemical and thermal analysis

(A) FTIR spectra of poplar and different CRM samples.

(B) FTIR spectra of different NCC samples.

(C) TG and DTG curves of CRM-180 and NCC-180.

(D) TG and DTG curves of CRM-240 and NCC-240.

The conclusion can also be further confirmed by the XPS results of the original poplar, CRM and NCC samples (Figure S1). The XPS spectrum of NCC sample exhibited a stronger intensity of O1s characteristic peak at 533.5 eV, indicating the elevated crystallinity of cellulose, whereas obvious shifts on the characteristic peak cannot be observed, which showed there was no obvious derivatization of cellulose during the NCC preparation process.

Thermal stability analysis

The difference in thermal stability between NCC and CRM was investigated by thermogravimetry, and the TG and derivative thermogravimetric (DTG) curves of CRM and NCC obtained at 180 °C and 240 °C are displayed in Figures 4C and 4D. The initial degradation temperature of both CRM-180 and CRM-240 was lower than that of the corresponding NCC (~250 °C vs. ~270 °C). This should be mainly because of the presence of non-cellulose components (especially hemicellulose) in the CRM. The degradation temperature of hemicellulose was lower than that of cellulose,[31] leading to lower initial degradation temperatures of the CRMs. In addition, the temperatures corresponding to the maximum degradation rate of both CRM-180 (322 °C) and CRM-240 (310 °C) were also lower than that of the corresponding NCC (331 °C); this may also be because of cellulose having a higher thermal stability than non-cellulose components.[32] These results confirm the better thermal stability of NCC than that of CRM.

XRD analysis

The XRD patterns of CRM at different temperatures featured strong diffraction peaks at 2θ = 14.9°, 16.4°, 22.5°, and 34.5°, corresponding to (1^{-}10), (110), (200), and (004) crystal planes of cellulose I, respectively (Figure 5A).[33] The results show that the fractionation process had no significant influence on the CRM crystalline structure, whereas the process at different temperatures did affect the CRM crystallinity (Figures 5B and S2, Supporting Information). The crystallinity data obtained by the Segal and peak deconvolution methods indicates that the increase in the treatment temperature positively affected the crystallinity; the CRM crystallinity calculated with the peak deconvolution method increased from 64.6 to 73.1% as the treatment temperature increased. It has been reported that the removal of lignin and hemicellulose can increase the CRM crystallinity.[34,35] In the current study, as the increase in the treatment temperature could

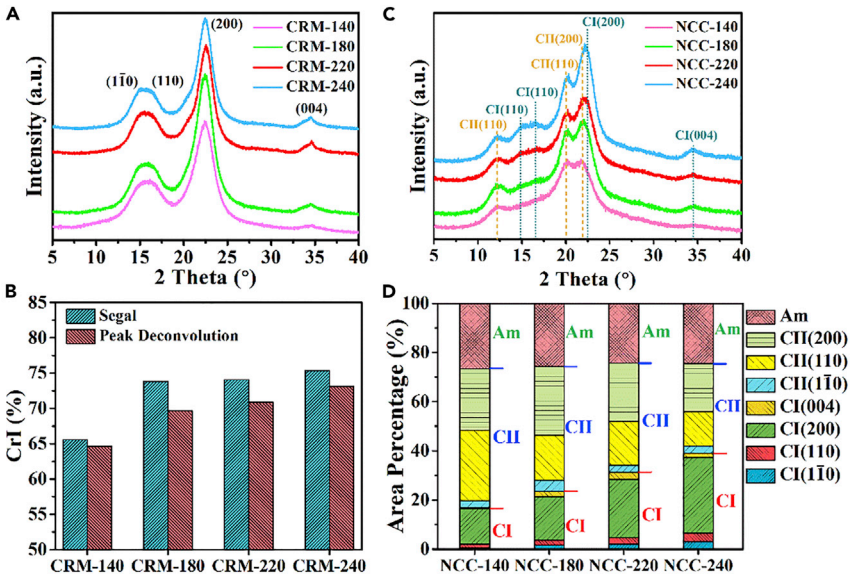

Figure 5. Results of crystal structure analysis

(A) X-ray diffractograms of CRMs obtained at different temperatures

(B) Crystallinity results of different CRM samples.

(C) X-ray diffractograms of different NCC samples.

(D) Area percentages of diffraction peaks in XRD patterns of NCC (CI: cellulose I; CII: cellulose II; Am: amorphous peaks).

facilitate the removal of lignin and hemicellulose, the fractionation process at higher temperatures led to higher CRM crystallinity.

The XRD patterns of different NCC samples confirmed the mixed crystal form of cellulose I and cellulose II (Figure 5C). Especially, the diffraction pattern of NCC-140 exhibited typical cellulose II diffraction peaks at $2\theta = 12.1°$, 20.0°, and 21.8°, which are attributed to the (1^{-}10), (110), and (200) crystal planes of cellulose II.[36] Characteristic diffraction peaks of cellulose I also appeared in the diffraction patterns of different NCC samples, including (1^{-}10), (110), (200), and (004) peaks.[33] The peak deconvolution analysis of the XRD patterns was conducted to investigate the effect of the raw material (CRM) on the crystalline structure of the as-prepared NCCs (Figures 5D and S3). The results indicate that the peak area percentage of cellulose I gradually rose as the CRM treatment temperature increased. In addition, the raw materials (i.e., CRM) showed limited influence on the crystallinity of the as-prepared NCC, and different NCC samples possessed a crystallinity of around 75%. Considering the different CRM lignin contents, it can be inferred that a low lignin content was beneficial to the retention of the cellulose I structure in NCC during the NCC preparation process with TPBH. As an organic base, TPBH could dissolve cellulose and transform the natural cellulose I structure into cellulose II. It also showed superior lignin solubility, and the presence of lignin in lignocellulosic materials was beneficial for TBPH to enter the cellulose, destroy the hydrogen bonding, and change the cellulose crystalline structure.[23,37] Consequently, the higher lignin content led to a larger change in the NCC crystalline form. The CRM with low lignin content possessed high crystallinity, which hindered the TBPH penetration into the cellulose, thus slowing down the crystal transition of NCC.

Optical microscopy analysis

To explore the dissolution process of CRM in TBPH solution, the dissolution processes of different CRM samples were observed via fluorescence microscopy and polarized light microscopy. The existence of lignin in the CRM/TBPH solution could produce a fluorescence effect, and it made the dissolution processes of CRM-140 and CRM-180 visible under the fluorescence microscope (Figure 6). The results indicate the relatively high lignin contents in CRM-140 and CRM-180, which were consistent with the fractionation results. For CRM-140, the rod-like structure was gradually destroyed in TBPH solution, the CRM particle size was reduced, and the surface became rough. Finally, CRM was separated into slender filaments, and the rapid lignin dissolution played an important role in the TPBH permeation and CRM deconstruction.[32] As

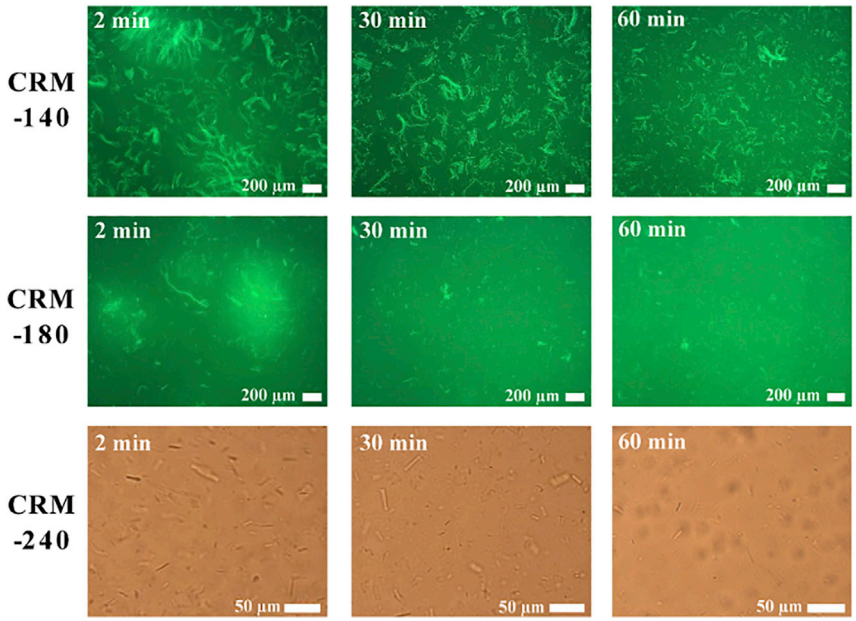

Figure 6. Fluorescence microscopy images of CRM dissolution in TBPH solution

the treatment temperature increased, both the CRM particle size and the lignin content decreased; thus, CRM-180 and CRM-240 exhibited less lignin dissolution and smaller size change than CRM-140. This phenomenon is a possible explanation for the different crystal forms of NCC prepared from the CRM raw materials with different lignin contents.

The polarized light microscopy results agreed with the fluorescence microscopy results (Figure 7), and CRM with a higher lignin content showed larger size change and deconstruction. In addition, partial cellulose

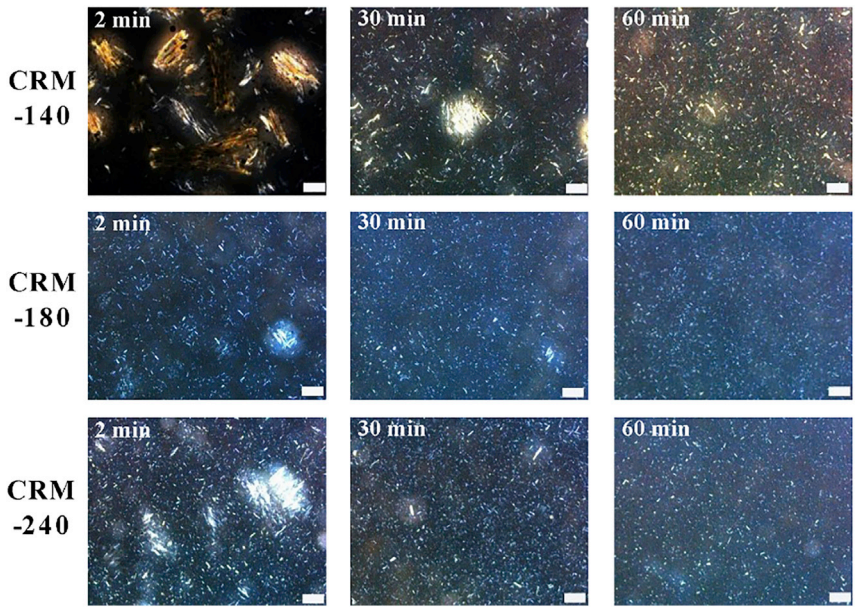

Figure 7. Polarized light microscopy images of CRM dissolution in TBPH solution (scale bar: 250 μm)

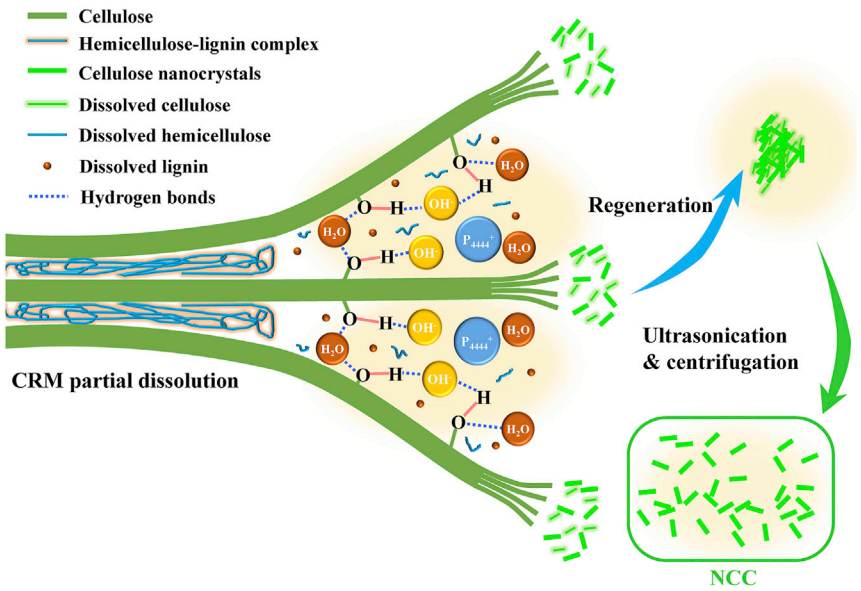

Figure 8. The proposed mechanism of NCC preparation from lignocellulosic biomass with TBPH solution

dissolution occurred in the TBPH solution, and CRM was finally decomposed into micron-sized particles. Therefore, NCC with a mixed crystal form of cellulose I and cellulose II could be obtained after regeneration and ultrasonication treatment.

Mechanism analysis

Based on the above results, a partial/selective dissolution mechanism for NCC preparation from lignocellulosic biomass with TBPH solution is proposed (Figure 8). The polarization and fluorescence results showed that the polymeric network structure of CRM was destroyed in the 40 wt % TBPH solution at 50 °C, and the CRM became loose, which promoted the penetration of OH^- and $[P_{4444}]^+$ ions into the CRM internal structure. The free OH^- interacted with the protons of the cellulose hydroxyl in CRM to form hydrogen bonds, whereas the free $[P_{4444}]^+$ attacked the oxygen atoms in the hydroxyl group.[38,39] Moreover, the electronegative α-methylene on the cation interacted with the carbon atom (C-1) on the cellulose through electrostatic or van der Waals forces to form the cellulose-$[P_{4444}]^+$ complex with polyelectrolyte properties.[40] Because of the synergistic effect of OH^- and $[P_{4444}]^+$ in TBPH, the hydrogen bonding network in cellulose was destroyed, which led to the swelling behavior of cellulose and further promoted the CRM dissolution. After the TBPH treatment of CRM, residual lignin and hemicellulose were selectively dissolved and removed, and the cellulose crystalline structure was partially converted to cellulose II during the cellulose partial dissolution process.[41] And the hydrogen bonding in cellulose was reconstructed to during the cellulose regeneration with the addition of water. Because the cellulose crystalline structure was not completely destroyed in the 60 min TBPH treatment process, the regenerated cellulose still contained cellulose I crystalline structure. Both the XRD results and microscopic analyses confirm these inferences. After ultrasonic and centrifugal treatment, the regenerated cellulose was uniformly dispersed in water to form NCC suspension (length: 50–200 nm, diameter: 3–13 nm). Therefore, in this study, bleaching-free, lignin-tolerant, high-yield NCC production was mainly attributed to the partial dissolution of cellulose and the selective dissolution and removal of other components (i.e., lignin and hemicellulose) in the TBPH system.

Conclusions

An integrated fractionation methodology for NCC preparation was investigated based on the catalytic fractionation, partial dissolution, and short-term ultrasonication of lignocellulosic biomass. Bleaching-free, lignin-tolerant, high-yield NCC production was achieved after lignin separation and hemicellulose conversion with the present strategy. The yield and crystalline structure of NCC can be regulated by

changing the lignin content in CRM. A partial/selective dissolution mechanism was proposed based on the microscopic study and the NCC characteristics. The presented strategy provided a promising way of biomass valorization and comprehensive lignocellulose utilization through combining integrated fractionation with NCC preparation.

Limitations of the study

The complex structure and variability of biomass feedstocks pose a challenge to the wide applicability of the present method in the NCC preparation. In this study, a representative biomass, poplar wood, was selected as the starting materials for the TBPH pretreatment, which is a kind of fast-growing wood with universal availability. Further studies are needed to improve the applicability of the present strategy according to the characteristics of different biomass feedstocks. In addition, the cost of the treatment system is another concern. The TBPH system used in this study possesses the advantages of low viscosity and high treatment efficiency, whereas it needs to solve the problem of high cost. The main solution is to recycle the TBPH system, which has been studied in relevant literature. Finally, how to scale up the treatment system is still an unsolved problem, which needs to be applied through industrial scale experiments.

STAR★METHODS

Detailed methods are provided in the online version of this paper and include the following:

- KEY RESOURCES TABLE
- RESOURCE AVAILABILITY
  - Lead contact
  - Materials availability
  - Data and code availability
- METHOD DETAILS
  - Catalytic fractionation process
  - NCC production process
  - Characterizations
- QUANTIFICATION AND STATISTICAL ANALYSIS

SUPPLEMENTAL INFORMATION

Supplemental information can be found online at https://doi.org/10.1016/j.isci.2022.105771.

ACKNOWLEDGMENTS

The authors are grateful for the support of the National Natural Science Foundation of China (32171703; 31760183), the Natural Science Foundation of Guangxi (2020GXNSFAA297028; 2016GXNSFCA380025), the Project Funded by China Postdoctoral Science Foundation (2017M620361) and the Scientific Research Foundation of Guangxi University (XGZ150513).

AUTHOR CONTRIBUTIONS

Z.L.: Methodology, Writing – original draft, Validation, Investigation; D.X.: Methodology, Writing – original draft, Validation, Investigation; W.Z.: Methodology, Investigation; H.W.: Methodology, Investigation; T.O.: Methodology, Validation, Investigation; J.S.: Methodology, Writing – review and editing; Y.W.: Methodology, Writing – review and editing; F.C.: Conceptualization, Methodology, Writing – origin draft, Writing – review and editing, Supervision, Funding acquisition.

DECLARATION OF INTERESTS

The authors declare that they have no known competing financial interests or personal relationships that could have appeared to influence the work reported in this paper.

Received: May 13, 2022
Revised: October 31, 2022
Accepted: December 6, 2022
Published: January 20, 2023

REFERENCES

1. Carrier, M., Windt, M., Ziegler, B., Appelt, J., Saake, B., Meier, D., and Bridgwater, A. (2017). Quantitative insights into the fast pyrolysis of extracted cellulose. ChemSusChem *10*, 3212–3224. https://doi.org/10.1002/cssc.201700984.

2. Yang, X., Biswas, S.K., Han, J., Tanpichai, S., Li, M.-C., Chen, C., Zhu, S., Das, A.K., and Yano, H. (2021). Surface and interface engineering for nanocellulosic advanced materials. Adv. Mater. *33*, e2002264. https://doi.org/10.1002/adma.202002264.

3. Xu, M., Wu, X., Yang, Y., Ma, C., Li, W., Yu, H., Chen, Z., Li, J., Zhang, K., and Liu, S. (2020). Designing hybrid chiral photonic films with circularly polarized room-temperature phosphorescence. ACS Nano *14*, 11130–11139. https://doi.org/10.1021/acsnano.0c02060.

4. Yue, Y., Wang, X., Han, J., Yu, L., Chen, J., Wu, Q., and Jiang, J. (2019). Effects of nanocellulose on sodium alginate/polyacrylamide hydrogel: mechanical properties and adsorption-desorption capacities. Carbohydr. Polym. *206*, 289–301. https://doi.org/10.1016/j.carbpol.2018.10.105.

5. Du, H., Parit, M., Liu, K., Zhang, M., Jiang, Z., Huang, T.S., Zhang, X., and Si, C. (2021). Engineering cellulose nanopaper with water resistant, antibacterial, and improved barrier properties by impregnation of chitosan and the followed halogenation. Carbohydr. Polym. *270*, 118372. https://doi.org/10.1016/j.carbpol.2021.118372.

6. Afra, E., and Mousavi, S.M.M. (2015). Preparation of cellulose nanofibrils from microcrystalline cellulose by high intensity ultrasonication and its applicability as reinforcement for paper. J. Biobased Mat. Bioenergy *9*, 561–566. https://doi.org/10.1166/jbmb.2015.1557.

7. Sarosi, O.P., Bischof, R.H., and Potthast, A. (2020). Tailoring pulp cellulose with electron beam irradiation: effects of lignin and hemicellulose. ACS Sustainable Chem. Eng. *8*, 7235–7243. https://doi.org/10.1021/acssuschemeng.0c02165.

8. Ditzel, F.I., Prestes, E., Carvalho, B.M., Demiate, I.M., and Pinheiro, L.A. (2017). Nanocrystalline cellulose extracted from pine wood and corncob. Carbohydr. Polym. *157*, 1577–1585. https://doi.org/10.1016/j.carbpol.2016.11.036.

9. Chen, Y.W., Lee, H.V., and Abd Hamid, S.B. (2017). Facile production of nanostructured cellulose from Elaeis guineensis empty fruit bunch via one pot oxidative-hydrolysis isolation approach. Carbohydr. Polym. *157*, 1511–1524. https://doi.org/10.1016/j.carbpol.2016.11.030.

10. Maity, S.K. (2015). Opportunities, recent trends and challenges of integrated biorefinery: Part I. Renew. Sustain. Energy Rev. *43*, 1427–1445. https://doi.org/10.1016/j.rser.2014.11.092.

11. Brinchi, L., Cotana, F., Fortunati, E., and Kenny, J.M. (2013). Production of nanocrystalline cellulose from lignocellulosic biomass: technology and applications. Carbohydr. Polym. *94*, 154–169. https://doi.org/10.1016/j.carbpol.2013.01.033.

12. Zhang, R., and Liu, Y. (2018). High energy oxidation and organosolv solubilization for high yield isolation of cellulose nanocrystals (CNC) from Eucalyptus hardwood. Sci. Rep. *8*, 16505. https://doi.org/10.1038/s41598-018-34667-2.

13. Zhang, Y., Hou, Q., Fu, Y., Xu, C., Smeds, A.I., Willför, S., Wang, Z., Li, Z., and Qin, M. (2018). One-step fractionation of the main components of bamboo by formic acid-based organosolv process under pressure. J. Wood Chem. Technol. *38*, 170–182. https://doi.org/10.1080/02773813.2017.1388823.

14. Tian, D., Guo, Y., Hu, J., Yang, G., Zhang, J., Luo, L., Xiao, Y., Deng, S., Deng, O., Zhou, W., and Shen, F. (2020). Acidic deep eutectic solvents pretreatment for selective lignocellulosic biomass fractionation with enhanced cellulose reactivity. Int. J. Biol. Macromol. *142*, 288–297. https://doi.org/10.1016/j.ijbiomac.2019.09.100.

15. Zhang, J., Elder, T.J., Pu, Y., and Ragauskas, A.J. (2007). Facile synthesis of spherical cellulose nanoparticles. Carbohydr. Polym. *69*, 607–611. https://doi.org/10.1016/j.carbpol.2007.01.019.

16. Park, N.-M., Choi, S., Oh, J.E., and Hwang, D.Y. (2019). Facile extraction of cellulose nanocrystals. Carbohydr. Polym. *223*, 115114. https://doi.org/10.1016/j.carbpol.2019.115114.

17. Cui, S., Zhang, S., Ge, S., Xiong, L., and Sun, Q. (2016). Green preparation and characterization of size-controlled nanocrystalline cellulose via ultrasonic-assisted enzymatic hydrolysis. Ind. Crop. Prod. *83*, 346–352. https://doi.org/10.1016/j.indcrop.2016.01.019.

18. Iskak, N.A.M., Julkapli, N.M., and Hamid, S.B.A. (2017). Understanding the effect of synthesis parameters on the catalytic ionic liquid hydrolysis process of cellulose nanocrystals. Cellulose *24*, 2469–2481. https://doi.org/10.1007/s10570-017-1273-2.

19. Abushammala, H., Krossing, I., and Laborie, M.-P. (2015). Ionic liquid-mediated technology to produce cellulose nanocrystals directly from wood. Carbohydr. Polym. *134*, 609–616. https://doi.org/10.1016/j.carbpol.2015.07.079.

20. Cruz, H., Fanselow, M., Holbrey, J.D., and Seddon, K.R. (2012). Determining relative rates of cellulose dissolution in ionic liquids through in situ viscosity measurement. Chem. Commun. *48*, 5620–5622. https://doi.org/10.1039/c2cc31487h.

21. Jiang, J., Carrillo-Enríquez, N.C., Oguzlu, H., Han, X., Bi, R., Saddler, J.N., Sun, R.-C., and Jiang, F. (2020). Acidic deep eutectic solvent assisted isolation of lignin containing nanocellulose from thermomechanical pulp. Carbohydr. Polym. *247*, 116727. https://doi.org/10.1016/j.carbpol.2020.116727.

22. Rojo, E., Peresin, M.S., Sampson, W.W., Hoeger, I.C., Vartiainen, J., Laine, J., and Rojas, O.J. (2015). Comprehensive elucidation of the effect of residual lignin on the physical, barrier, mechanical and surface properties of nanocellulose films. Green Chem. *17*, 1853–1866. https://doi.org/10.1039/c4gc02398f.

23. Abe, M., Yamanaka, S., Yamada, H., Yamada, T., and Ohno, H. (2015). Almost complete dissolution of woody biomass with tetra-n-butylphosphonium hydroxide aqueous solution at 60 °C. Green Chem. *17*, 4432–4438. https://doi.org/10.1039/C5GC00646E.

24. Cheng, F., Sun, J., Wang, Z., Zhao, X., and Hu, Y. (2019). Organosolv fractionation and simultaneous conversion of lignocellulosic biomass in aqueous 1, 4-butanediol/acidic ionic-liquids solution. Ind. Crop. Prod. *138*, 111573. https://doi.org/10.1016/j.indcrop.2019.111573.

25. Wildschut, J., Smit, A.T., Reith, J.H., and Huijgen, W.J.J. (2013). Ethanol-based organosolv fractionation of wheat straw for the production of lignin and enzymatically digestible cellulose. Bioresour. Technol. *135*, 58–66. https://doi.org/10.1016/j.biortech.2012.10.050.

26. Brito, B.S.L., Pereira, F.V., Putaux, J.-L., and Jean, B. (2012). Preparation, morphology and structure of cellulose nanocrystals from bamboo fibers. Cellulose *19*, 1527–1536. https://doi.org/10.1007/s10570-012-9738-9.

27. Nagatani, M., Tsurumaki, A., Takamatsu, K., Saito, H., Nakamura, N., and Ohno, H. (2019). Preparation of epoxy resins derived from lignin solubilized in tetrabutylphosphonium hydroxide aqueous solutions. Int. J. Biol. Macromol. *132*, 585–591. https://doi.org/10.1016/j.ijbiomac.2019.03.152.

28. Saher, S., Saleem, H., Asim, A.M., Uroos, M., and Muhammad, N. (2018). Pyridinium based ionic liquid: a pretreatment solvent and reaction medium for catalytic conversion of cellulose to total reducing sugars (TRS). J. Mol. Liq. *272*, 330–336. https://doi.org/10.1016/j.molliq.2018.09.099.

29. Bian, H., Chen, L., Dai, H., and Zhu, J.Y. (2017). Integrated production of lignin containing cellulose nanocrystals (LCNC) and nanofibrils (LCNF) using an easily recyclable di-carboxylic acid. Carbohydr. Polym. *167*, 167–176. https://doi.org/10.1016/j.carbpol.2017.03.050.

30. Le Moigne, N., and Navard, P. (2010). Dissolution mechanisms of wood cellulose fibres in NaOH–water. Cellulose *17*, 31–45. https://doi.org/10.1007/s10570-009-9370-5.

31. Lazko, J., Sénéchal, T., Bouchut, A., Paint, Y., Dangreau, L., Fradet, A., Tessier, M., Raquez, J.M., and Dubois, P. (2016). Acid-free extraction of cellulose type I nanocrystals using Brønsted acid-type ionic liquids. Nanocomposites *2*, 65–75. https://doi.org/10.1080/20550324.2016.1199410.

32. Johar, N., Ahmad, I., and Dufresne, A. (2012). Extraction, preparation and characterization of cellulose fibres and nanocrystals from rice husk. Ind. Crop. Prod. *37*, 93–99. https://doi.org/10.1016/j.indcrop.2011.12.016.

33. Azubuike, C.P., Rodríguez, H., Okhamafe, A.O., and Rogers, R.D. (2012). Physicochemical properties of maize cob cellulose powders reconstituted from ionic liquid solution. Cellulose *19*, 425–433. https://doi.org/10.1007/s10570-011-9631-y.

34. Chen, W., Yu, H., Liu, Y., Chen, P., Zhang, M., and Hai, Y. (2011). Individualization of cellulose nanofibers from wood using high-intensity ultrasonication combined with chemical pretreatments. Carbohydr. Polym. *83*, 1804–1811. https://doi.org/10.1016/j.carbpol.2010.10.040.

35. Alemdar, A., and Sain, M. (2008). Isolation and characterization of nanofibers from agricultural residues – wheat straw and soy hulls. Bioresour. Technol. *99*, 1664–1671. https://doi.org/10.1016/j.biortech.2007.04.029.

36. Oudiani, A.E., Chaabouni, Y., Msahli, S., and Sakli, F. (2011). Crystal transition from cellulose I to cellulose II in NaOH treated Agave americana L. Carbohydr. Polym. *86*, 1221–1229. https://doi.org/10.1016/j.carbpol.2011.06.037.

37. Nguyen, M.N., Kragl, U., Michalik, D., Ludwig, R., and Hollmann, D. (2019). The effect of additives on the viscosity and dissolution of cellulose in tetrabutylphosphonium hydroxide. ChemSusChem *12*, 3458–3462. https://doi.org/10.1002/cssc.201901316.

38. Abe, M., Fukaya, Y., and Ohno, H. (2012). Fast and facile dissolution of cellulose with tetrabutylphosphonium hydroxide containing 40 wt% water. Chem. Commun. *48*, 1808–1810. https://doi.org/10.1039/c2cc16203b.

39. Zhong, C., Cheng, F., Zhu, Y., Gao, Z., Jia, H., and Wei, P. (2017). Dissolution mechanism of cellulose in quaternary ammonium hydroxide: revisiting through molecular interactions. Carbohydr. Polym. *174*, 400–408. https://doi.org/10.1016/j.carbpol.2017.06.078.

40. Yu, C.A., Gu, L.Q., Lin, Y.Z., and Yu, L. (1985). Effect of alkyl side chain variation on the electron-transfer activity of ubiquinone derivatives. Biochemistry *24*, 3897–3902. https://doi.org/10.1021/bi00336a013.

41. Cheng, F., Zhao, P., Ouyang, T., Sun, J., and Wu, Y. (2021). Comprehensive utilization strategy of cellulose in a facile, controllable, high-yield preparation process of cellulose nanocrystals using aqueous tetrabutylphosphonium hydroxide. Green Chem. *23*, 1805–1815. https://doi.org/10.1039/d0gc04370b.

42. Cheng, F., Zhao, X., and Hu, Y. (2018). Lignocellulosic biomass delignification using aqueous alcohol solutions with the catalysis of acidic ionic liquids: a comparison study of solvents. Bioresour. Technol. *249*, 969–975. https://doi.org/10.1016/j.biortech.2017.10.089.

STAR★METHODS

KEY RESOURCES TABLE

REAGENT or RESOURCE	SOURCE	IDENTIFIER
[Bmim][HSO_4]	Lanzhou Institute of Chemical Physics	Chinese Academy of Sciences
GVL and TBPH	Shanghai Aladdin	
Ultrasonic Processor	Nanjing Immanuel Instrument	Ymnl-1800Y
Scanning Electron Microscope	Hitachi	Hitachi S-3400N
Transmission Electron Microscopy	Hitachi	HT7700 TEM
FT-IR spectra	Thermo Fisher Scientific	Nicolet iS 502 FT-IR
XRD Analyzer	Rigaku	SMARTLAB3KW
Fluorescence Microscope	Carl Zeiss	IMAGER.Z2
Polarized Light Microscopy	Carl Zeiss	Axio Vert. A1
TG analysis	Shimadzu	DTG-60H

RESOURCE AVAILABILITY

Lead contact

Further information and requests for resources should be directed to and will be fulfilled by the lead contact, Fangchao Cheng (fangchaocheng@gxu.edu.cn).

Materials availability

This study did not generate unique reagents.

Data and code availability

- All data reported in this paper will shared by the lead contact upon request.
- This study did not generate original code.
- Any additional information required to reanalyze the data reported in this work is available from the lead contact upon reasonable request.

METHOD DETAILS

Catalytic fractionation process

In a 50-mL stainless steel reactor, 2 g poplar powder was added and mixed with 20 mL aqueous GVL solution (16 mL GVL and 4 mL water) containing 0.67 g [Bmim][HSO_4]. The reactor was heated in an oil bath for 30 min. After the reaction liquor was cooled to room temperature, it was filtered with an organic filter (0.45 μm) under vacuum to separate the CRMs. Water was added into the filtrate, and the mixture was allowed to stand for 24 h to regenerate lignin. The obtained CRM and lignin were washed with ethanol and water, respectively, for three to five times and dried at 60 °C for 24 h, respectively. The CRM and lignin yields were the ratios of their mass to the mass of the original poplar powder. The delignification rate was calculated according to Equation 1:

$$\text{Delignification rate} = (M_P \times L_P - M_C \times L_C) / (M_P \times L_P) \times 100\%, \quad \text{(Equation 1)}$$

where M_P and M_C represent the mass of poplar powder and CRM, respectively, and L_P and L_C represent the lignin contents in poplar powder and CRM, respectively.

A series of treatment temperatures, including 120 °C, 140 °C, 160 °C, 180 °C, 200 °C, 220 °C, and 240 °C, were adopted in this study to achieve CRMs of different lignin contents. The experiment was repeated three times at each temperature, and the fractionation results were averaged. The CRM obtained at the specific temperature was named CRM-T (e.g., CRM-120), where T represents the temperature value.

NCC production process

In a typical run, 0.05 g CRM was immersed in 1 g of 40 wt % TBPH solution, and the mixture was stirred at 50 °C for 1 h. Then, 10 mL water was added to the mixture to regenerate the partially dissolved cellulose. The regenerated cellulose was washed with water by vacuum filtration for three to five times. After the final filtration, 50 mL water was mixed with the regenerated cellulose, and then the mixture was treated with an ultrasonic processor (Ymnl-1800Y, Nanjing Immanuel Instrument Equipment Co. LTD, China) at a power of 1600 W for 240 s. The mixture was then centrifuged at 8000 r/min for 5 min, and the supernatant was the NCC suspension, which was then filtered with an organic filter (0.22 μm) under vacuum to collect the obtained NCC. The experiment was repeated three times for each CRM sample, and the NCC yield was calculated using Equation 2. The mean value of the three replicates were adopted to present the results of NCC preparation. The NCC prepared from CRM-X was named NCC-X (e.g., NCC-120):

$$Y_{NCC} = M_N/M_C \times 100\%, \quad \text{(Equation 2)}$$

where M_N and M_C represent the mass of NCC and CRM, respectively. The NCC extraction rate was calculated using Equation 3:

$$\begin{aligned} NCC\ \ extraction\ \ rate &= M_N/M_P \times 100\%, \\ &= (M_N/M_C) \times (M_C/M_P) \times 100\%, \\ &= Y_{NCC} \times Y_{CRM} \times 100\%, \end{aligned} \quad \text{(Equation 3)}$$

where M_N, M_C, and M_P represent the mass of NCC, CRM, and poplar powder, respectively, and Y_{NCC} and Y_{CRM} denote the NCC and CRM yields, respectively. The overall production process for NCC is summarized in Figure 1.

Characterizations

The X-ray diffraction (XRD) patterns of CRM and NCC were determined using a SMARTLAB3KW X-ray diffractometer (Rigaku Corporation, Japan) equipped with Cu-Kα radiation source in the range 2θ = 5–40° at a scanning rate of 5°/min in steps of 0.01°. The peak deconvolution method was used to determine the crystallinity index (*CrI*) with Equation 4:[36]

$$CrI\,(\%) = (A_1 - A_2)/A_1 \times 100\%, \quad \text{(Equation 4)}$$

where A_1 and A_2 denote the total area of the diffractogram and the area of amorphous peak, respectively.

The relative crystallinity of CRM was also calculated with Equation 5 according to the Segal method:

$$CrI\,(\%) = ((I_{200} - I_{am})/I_{200}) \times 100\%, \quad \text{(Equation 5)}$$

where I_{200} is the peak intensity of the diffraction peak associated with the (200) plane, and I_{am} is the diffraction intensity of the amorphous cellulose fraction at 2θ = 18°.

The Fouriertransform infrared (FT-IR) spectra of CRM and NCC were collected with a Nicolet iS 502 FT-IR spectrometer (Thermo Fisher Scientific Corporation, USA) over the range of 500–4000 cm^{-1}, with 16 scans at a resolution of 4 cm^{-1}.

Thermogravimetric (TG) analysis was performed using a DTG-60H TG analyzer (Shimadzu Corporation, Japan) with a temperature range of 25°C-550°Cat a heating rate of 10 °C/min. The temperature was maintained for 10 min after heating to 550 °C.

The morphologies of CRMs obtained at different temperatures were observed with a Hitachi S-3400N scanning electron microscope (Hitachi Corporation, Japan) at an accelerated voltage of 15 kV.

An NCC suspension with a concentration of 0.08% was added to a copper mesh covered with carbon film, and negative staining was performed with 2 wt % phosphotungstic acid solution for 30 min to prepare the transmission electron microscopy (TEM) sample. After natural drying, the morphology of the sample was observed using an HT7700 TEM (Hitachi Corporation, Japan) with an acceleration voltage of 100 kV. The dimensions of NCC sample were analyzed in a Nano Measurer software with three TEM images for each sample, and the length and diameter data of 200 NCC particles was collected in each TEM image.

The dissolution behavior of CRM in TBPH solution was observed using an IMAGER.Z2 fluorescence microscope (Carl Zeiss Corporation, Germany) and an Axio Vert. A1 polarized microscope (Carl Zeiss Corporation, Germany).

The lignin contents of CRM samples were determined via a previously reported method.[42] First, 0.2 g CRM was immersed in 4 mL of 72 wt % H_2SO_4 solution and stirred at room temperature for 4 h, and then 112 mL water was added to dilute the H_2SO_4 solution. The solution was then refluxed for 2 hat 105 °C. The acid-insoluble lignin was obtained through vacuum filtration and drying, and the amount of acid-soluble lignin was determined using a UV spectrophotometer at 205 nm.

QUANTIFICATION AND STATISTICAL ANALYSIS

All experiments were conducted in triplicates to obtain the CRM and NCC yields and their standard deviation. The NCC dimensions were analyzed with three TEM images for each sample, and 200 NCC particles was collected in each TEM image.